



Assessment of land use and land cover, water nutrient and metal concentration related to illegal mining activities in an Austral semi-arid river system: A remote sensing and multivariate analysis approach

Thandekile Dube^{a,*}, Timothy Dube^a, Tatenda Dalu^{b,*}, Siyamthanda Gxokwe^a, Thomas Marambanyika^c

^a Institute for Water Studies, Department of Earth Science, University of the Western Cape, Bellville 7535, South Africa

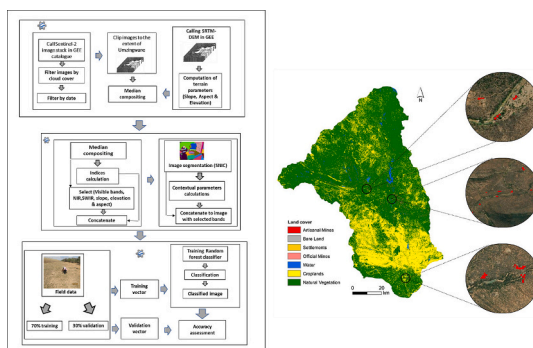
^b Aquatic Systems Research Group, School of Biology and Environmental Sciences, University of Mpumalanga, Nelspruit 1200, South Africa

^c Department of Geography, Environmental Sustainability and Resilience Building, Midlands State University, Gweru, Zimbabwe

HIGHLIGHTS

- LULC analysis revealed seven classes within the Umzingwane River Catchment.
- LULC analysis showed artisanal mines are predominantly located along rivers.
- River ecosystem health was found to be significantly different across river systems.
- Nutrients and metals in the river water were not highly correlated.
- Study provides a foundational understanding of river health status.

GRAPHICAL ABSTRACT



ARTICLE INFO

Editor: Damia Barcelo

Keywords:

Artisanal mines
Dryland rivers
Mercury
River health
Water contamination

ABSTRACT

The mining sector in various countries, particularly in the sub-Saharan African region, faces significant impact from the emergence of small-scale unlicensed artisanal mines. This trend is influenced by the rising demand and prices for minerals, along with prevalent poverty levels. Thus, the detrimental impacts of these artisanal mines on the natural environment (i.e., rivers) have remained poorly understood particularly in the Zimbabwean context. To understand the consequences of this situation, a study was conducted in the Umzingwane Catchment, located in southern Zimbabwe, focusing on the variations in water nutrient and metal concentrations in rivers affected by illegal mining activities along their riparian zones. Using multi-year Sentinel-2 composite data and the random forest machine learning algorithm on the Google Earth Engine cloud-computing platform, we mapped the spatial distribution of illegal mines in the affected regions and seven distinct land use classes, including artisanal mines, bare surfaces, settlements, official mines, croplands, and natural vegetation, with an acceptable overall and class accuracies of $\pm 70\%$ were identified. Artisanal mines were found to be located along rivers and this was attributed to their large water requirements needed during the mining process. The water quality analysis revealed elevated nutrient concentrations, such as ammonium and nitrate (range $0.10\text{--}20.0\text{ mg L}^{-1}$), which

* Corresponding authors.

E-mail addresses: 4206001@myuwc.ac.za (T. Dube), dalutatenda@yahoo.co.uk (T. Dalu).

<https://doi.org/10.1016/j.scitotenv.2023.167919>

Received 22 June 2023; Received in revised form 13 October 2023; Accepted 16 October 2023

Available online 23 October 2023

0048-9697/© 2023 Published by Elsevier B.V.

could be attributed to mine drainage from the use of ammonium nitrate explosives during mining activities. Additionally, the prevalence of croplands in the area may have potentially contributed to increased nutrient concentrations. The principal component analysis and hierarchical cluster analysis revealed three clusters, with one of these clusters showing parameters like Ca, Mg, K, Hg and Na, which are usually associated with mineral gypsum found in the drainage of artisanal mines in the selected rivers. Cluster 2 consisted of B, Cu, Fe, Pb, and Mn, which are likely from the natural environment and finally, cluster 3 contained As, Cd, Cr, and Zn, which were likely associated with both legal and illegal mining operations. These findings provide essential insights into the health of the studied river system and the impacts of human activities in the region. They further serve as a foundation for developing and implementing regulatory measures aimed at protecting riverine systems, in line with sustainable development goal 15.1 which focuses on preserving and conserving terrestrial and inland freshwater ecosystems, including rivers. By acting on this information, authorities can work towards safeguarding these vital natural resources and promoting sustainable development in the area.

1. Introduction

Mining, a significant economic driver, plays a pivotal role in many countries worldwide (Liang et al., 2022; Omotehinse and De Tomi, 2023). This industry generates substantial revenue, benefiting millions of people across regions such as sub-Saharan Africa, South and Central America, and Asia (Hodge et al., 2022). One notable example in sub-Saharan Africa is the Democratic Republic of Congo where mined minerals account for 81 % of the total exports, making a substantial contribution to their economy (Hodge et al., 2022). Whereas other countries such as Botswana and Mongolia, mining sector contribute between 80 % and 90 % towards their annual exports. However, the mining sector in different sub-Saharan African countries are heavily impacted by the sprouting illegal mines and/or small scale unlicensed artisanal mines which continued to grow and doubled between 1999 and 2014 (Ericsson and Löf, 2019; Hodge et al., 2022). The growth can be attributed to the global increase in mineral prices, political and socio-economic challenges. The estimated percentage of people in Africa who directly earn a living from artisanal mining varies widely across different regions and countries (Dalu et al., 2018, 2021). However, it is generally recognised that a significant portion of the population in certain areas relies on artisanal mining for their livelihoods and about 20–30 % of Africa's population is engaged in artisanal mining activities (Seccatore et al., 2014; García et al., 2015). According to Duncan (2020), countries in Africa are grappling with significant environmental and social issues that can be attributed to unregulated illegal mining activities. Whereas Nasirudeen and Allan (2014) in Ghana specifically highlighted that illegal small-scale mining plays a significant role in compromising sound environmental practices within the country's mining industry.

Illegal mines or small-scale unlicensed artisanal gold mines are typically characterised by randomly dug open pits with variable sizes ranging between 37 m² and 372 m², while their depths range between 9 m and 18 m (Kessey and Arko, 2013). These types of mines typically employ basic exploratory tools and methods, operated by unskilled personnel who often lack knowledge about the harmful consequences of their mining activities on human livelihoods and the environment, including water resources (Owusu-Boateng and Kumi-Aboagye, 2013). Illegal mining operations have high water requirements for gold ore washing and are predominantly situated in riparian zones adjacent to surface water bodies such as rivers, lakes, wetlands, and streams. Consequently, these illegal mines frequently release untreated effluents containing hazardous chemicals (e.g., mercury (Hg), cyanide (CN), cadmium (Cd)) and heavy metals (e.g., chromium (Cr), lead (Pb)) into water bodies, resulting in contamination and significant adverse impacts on the natural environment (Dalu et al., 2017a, 2017b, 2022). These activities collectively contribute to the contamination of aquatic ecosystems. Therefore, strong regulatory measures are imperative to effectively control and mitigate the growing prevalence of illegal mining activities, thereby halting their detrimental effects on both human livelihoods and the environment.

The development of regulatory measures to control the emergence

and escalating impact of illegal mines on human livelihoods and the environment, relies on understanding the extent of their environmental impact and their consequences across large spatial scales and systems. Despite the reported growth of illegal artisanal mines in recent years, there is a lack of comprehensive reporting on the adverse impacts they have on the environment, especially water resources, at both local and broader spatial extents within southern Africa (Stoudmann et al., 2016; Amuah et al., 2021; Quarm et al., 2022). Given the increase in illegal mining activities in different regions and the recognised negative effects they have on the environment and society, it is crucial to have a comprehensive understanding of the extent of these illegal mining activities. Thus, such studies are essential for developing effective strategies to control the growth and emergence of illegal mines and regulate those already in existence.

This study aimed to assess the extent of variation in water nutrient and metal concentrations in semi-arid river systems affected by riparian illegal gold mining in the Umzingwane River catchment, southern-western Zimbabwe. We further mapped the spatial distribution of illegal gold mines in relation to other land use and land cover classes using multi-year Sentinel-2 satellite data and advanced machine learning algorithms in the Google Earth Engine platform. We hypothesised that river systems exposed to greater riparian activities associated with artisanal mining would exhibit elevated heavy metal concentrations (e.g., Cd, Hg), and other associated elements (e.g., arsenic (As), K, Na, Mg), compared to river systems with few or no illegal gold mining activities within their catchments.

2. Materials and methods

2.1. Study area

The study was conducted in the Umzingwane River Catchment (22.18694°S 29.92556°E) in the south-western part of Zimbabwe (Fig. 1). The catchment covers a total surface area of about 15,695 km². For this study, the Upper Umzingwane River sub-catchment which covers approximately 2138 km² was sampled for water quality assessment. The area receives variable rainfall, with mean annual precipitation of 300 mm per year in the southern region while the northern region receives about 635 mm per year (Maviza and Ahmed, 2020). Evapotranspiration rates in Umzingwane River catchment ranges from 1800 mm to 2000 mm, increasing towards the north-south directions. The mean annual minimum and maximum temperatures are 5 °C and 30 °C, respectively (Chisadza et al., 2023). The surface elevation range is 300 mm to 550 mm, with an average elevation of 1160 m above sea level (Sibanda et al., 2020). The dominant vegetation include the savannah rangeland woodlands characterised by *Brachystegia spiciformis*, *Colophospermum mopane*, *Terminalia spp.*, *Acacia spp.*, and *Combretum spp.*. In addition to the savannah rangelands species, there is also a presence of some grassland species such as *Hyparrhenia filipendula* and *Heteropogon contortus* (Mapaure and McCartney, 2001). The geology of the catchment is characterised by the greenstone belt underlain by the granitic terrains for the upper part of the catchment, while the lower part is

characterised by Limpopo belt gneisses and Karoo basalt (Ashton et al., 2001). The Umzingwane River catchment is characterised by variable land use and land cover (LULC) which includes agricultural activities (i.e., commercial and subsistence farming), game reserves or private safari operations, recreational activities, gold mining (i.e., legal and illegal), and fishing (Chisadza et al., 2023).

2.2. Ground control points collection

The collection of ground truth points (i.e., in-situ land cover sample points) representing the geographical locations of different land cover classes in Table 1 was carried out between 24 September and 9 October 2022. A total of 1182 ground truth points were surveyed. Out of these, 682 points were collected during field visits, while an additional 500 points were generated from a high-resolution Google Earth image coinciding with the remotely sensed images used in this study. The field data collection of the ground truth land cover location points utilised a handheld geographical positioning systems (GPS) with an error margin of <3.25 m, following a stratified random sampling approach. To ensure comprehensive coverage, the catchment was divided into 14 quadrants (2 km × 2 km), spaced 2 km apart to avoid overlaps in the collected points. At least 50 points were collected in each quadrant, considering the heterogeneity of land cover classes observed. The collected data from the points, both field and Google Earth-derived, were randomly split into training (70 %) and validation (30 %) sets and were then used

Table 1

Ground control points per land cover class.

Cover classes	Ground truth points per class	Training points per class	Validation points per class
Artisanal mines	44	31	13
Bare surface	122	85	37
Settlements	92	64	28
Official mines	75	53	22
Water	154	108	46
Croplands	256	179	77
Natural vegetation	437	306	131

in the Google Earth Engine (GEE) cloud-computing platform to train and validate the random forest machine learning model for land use and land cover analysis. Additionally, water samples were collected from the central (i.e., mainstem river) and littoral zones of the Umzingwane, Insiza, Msthabezi and Inyankuni rivers within the studied catchment. These rivers were selected because of the identified presence of artisanal mines based on the LULC analysis results. The locations of the sampling points are highlighted in Fig. 1.

2.3. Surface water sampling

The study sites were randomly selected along the selected rivers

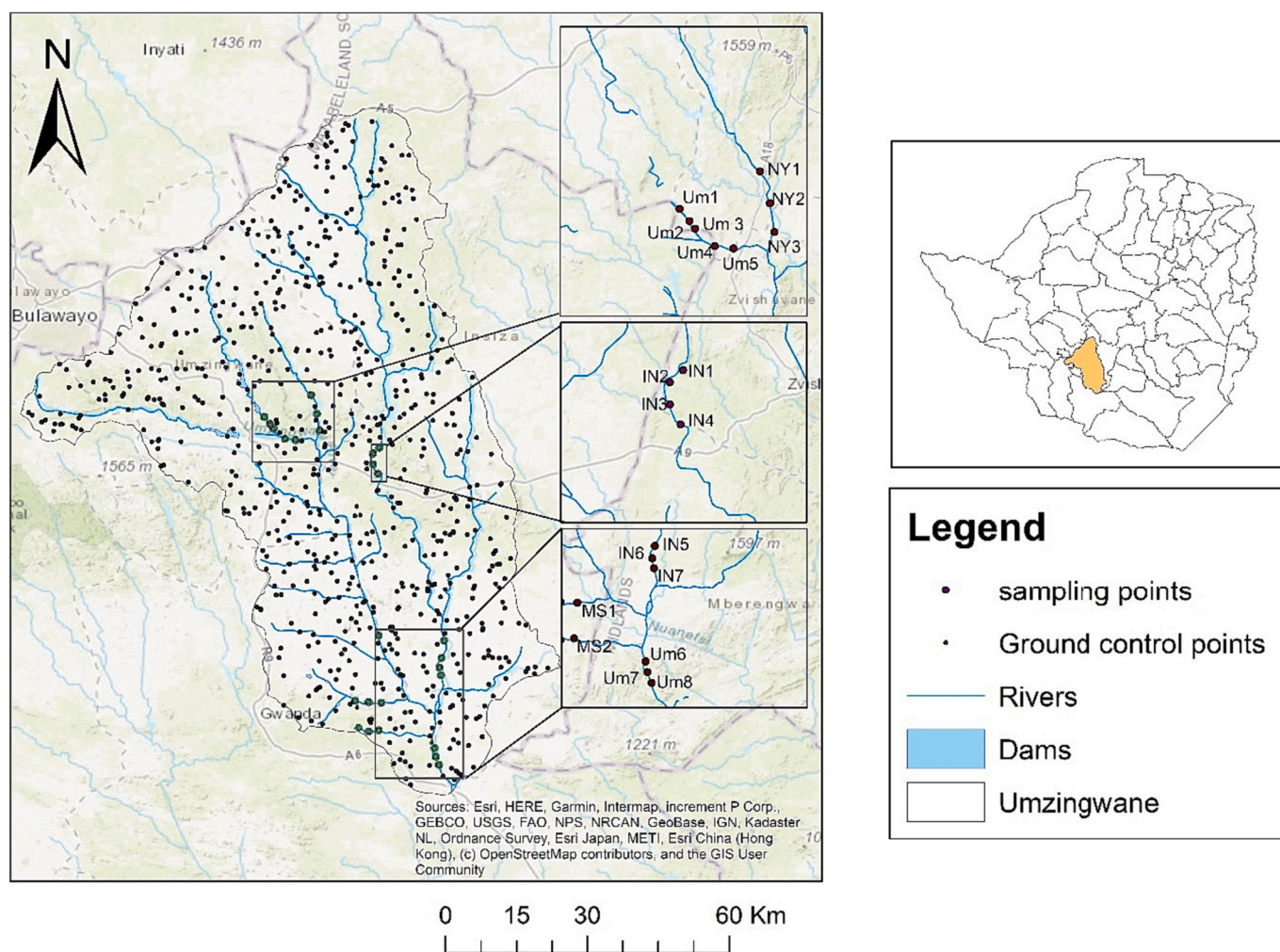


Fig. 1. Locality of Umzingwane River Catchment in Zimbabwe highlighting the ground control points representing different land cover classes in the catchment and environmental variable sampling sites. Abbreviations for sites and corresponding numbers indicate sites: Um – Umzingwane River, In – Insiza River, NY – Nyankuni River, MS – Msthabezi.

based on the close proximity to the artisanal mines. Twenty samples were collected following a standard grab sampling approach using 500 mL glass containers during a single sampling campaign conducted on the 13th of October 2022. During the collection of the samples, a 500 mL glass container was rinsed three times using the water from the sample point, then a water sample was collected at a depth of 20–30 cm in the pelagic column according to [Laxen and Harrison \(1981\)](#). In brief, water samples were collected from the two riparian zones and the mainstem channel before being mixed together to form an integrated water

sample. The bottle was tightly sealed making sure that no air bubbles were present and then stored on ice before sample processing in the laboratory.

2.4. Remote sensing of land use and land cover analysis

For the analysis of LULC, pre-processed Sentinel-2 Level 1C cloud-free images from the GEE catalogue were utilised. The processing steps for the Sentinel-2 data are depicted in [Fig. 2](#). The study specifically

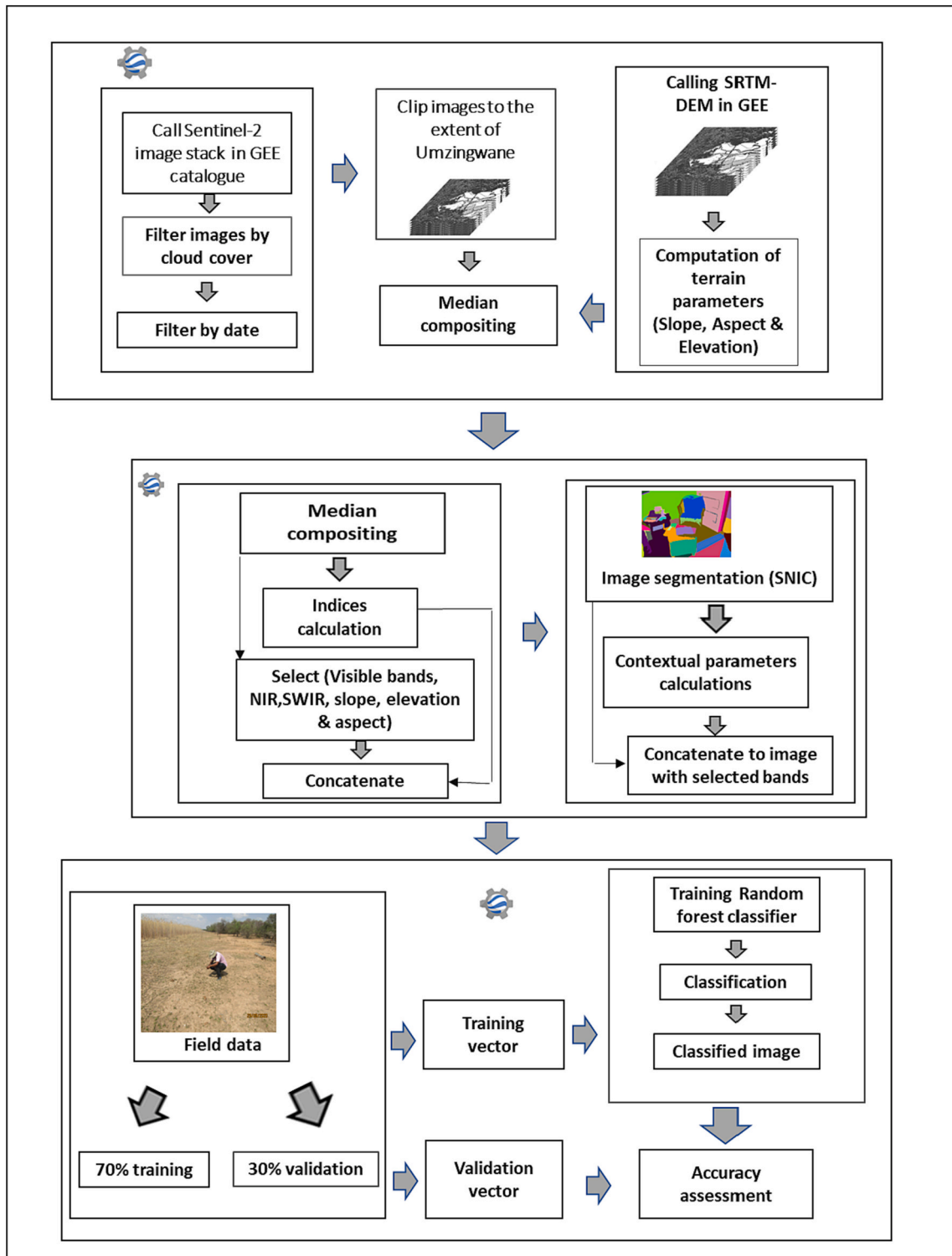


Fig. 2. Conceptual framework applied for remote sensing data analysis and land use and land cover change (LULC) classifications in this study.

clipped the obtained images to the extent of the Umzingwane River catchment and filtered them by date, focusing on images captured between 1 and 3 August 2022, which coincided with the field data collection period. To create a representative composite image for the entire period while minimising atmospheric influences, the median composite algorithm was applied to a stack of 66 images obtained from the filtering process. This algorithm computes the median value of corresponding bands and pixels across the image stack. The resulting composite image effectively captures the overall conditions during the specified time frame and mitigates the effects of shadows and cloud cover. Subsequently, water and vegetation indices were computed using the median composite image, including the Normalized Difference Vegetation Index (NDVI) and Modified Normalized Difference Water Index (MNDWI).

The NDVI serves to quantify vegetation greenness and distinguish vegetated areas from non-vegetated ones, making it a valuable tool for this study (McFeeters, 1996). The MNDWI is useful in enhancing water features and suppressing the built-up, vegetative and soil noises, thus minimising the spectral mixing between these classes and water during the classification process (Xu, 2006). It is for that reason, the MNDWI was used in this study. In addition to the indices, terrain parameters (*i.e.*, elevation, slope, aspect) were computed using a 30 m resolution Shuttle Radar Topographic Mission Digital Elevation Model (SRTM-DEM) obtained from the GEE catalogue. These were computed because, they can assist in segregating open pit artisanal mines, formal mines, zone of depressions as well as generally flats and sloppy surfaces. The indices and terrain parameters were then concatenated to the composite image with only near-infrared (NIR) band, visible bands (*i.e.*, red, green, blue) and shortwave infrared (SWIR) bands and used in image classification in the GEE cloud-computing platform using the object-based random forest (RF) machine learning algorithm. The RF algorithm is an ensemble classifier comprising of many different trees generated from a random set of input parameters (Simioni et al., 2020). Each tree cast a unit vote to the popular class, the class with most votes is classified as that feature of interest. The algorithm was chosen because of its superiority among other machine learning algorithm in various LULC studies (*e.g.*, Dzurume et al., 2021; Gxokwe et al., 2021; Thamaga et al., 2022). The initial phase to object-based RF implementation was image segmentation. This involved the partitioning of the image with concatenated indices and terrain parameters into equal segments based on a specific set criterion, using a simple non-iterative clustering (SNIC) algorithm in GEE.

The SNIC was chosen because it is simple, memory efficient and can maintain connectivity between pixels after it has been implemented (Achanta and Süstrunk, 2017). During the implementation of SNIC, centroids were initiated on a regular gridded image, then individual pixels were merged based on the shorted distance of each pixel to the centroid in five-dimensional space of colour and coordinates. The outputs were super pixels which were added onto the concatenated image and their contextual (*i.e.*, area, texture, perimeter, height) parameters were individually computed, and added on the concatenate image and the image was subjected to RF model. During the implementation of the RF model, the 70 % random split of the ground truth data was utilised in training the model. When training the RF model, the grid search values for mtree and mtry parameters were varied by 500 to 10 000 and 1 to 5, respectively. The intervals for mtree parameters were 500, and optimum mtree and mtry values were used (*i.e.*, 5000, 4) as input parameters to the RF model to classify the concatenate image.

2.5. Random forest model validation

To validate the RF model, three error matrices were used, and these included overall accuracy (OA), producer's accuracy (PA) and user's accuracy (UA). The OA measures the proportion of the correctly classified reference points, while PA measures the probability that a certain feature on the ground is correctly shown on the map, and UA gives an

indication of how often the class on a map represents what is on the ground (Mtengwana et al., 2020; Gxokwe et al., 2022). When implanting the above-mentioned error matrices in GEE, the 30 % randomly split data was imported in GEE and used to sample regions corresponding to those points, and these were used to compute an error matrix for the model which was later used to compute, OA, PA and UA. In addition to these matrices, multi-probability approach in GEE was used to establish the most significant variables and their influence in the model.

2.6. Water metal concentrations analysis

All metal and nutrient analysis was carried out in a South African National Accreditation System (SANAS) certified laboratory: WaterLab (Pretoria). For cation elements (B, Ca, K, Mg, Na) and heavy metals (As (Detection Limit (DL) – 0.007 mg L⁻¹), Cd (DL – 0.00015 mg L⁻¹), Cr (DL – 0.0007 mg L⁻¹), Cu (DL – 0.0005 mg L⁻¹), Fe (DL – 0.0001 mg L⁻¹), Hg (DL – 0.0003 mg L⁻¹), Mn (DL – 0.0001 mg L⁻¹), Pb (DL – 0.0005 mg L⁻¹), Zn (DL – 0.0002 mg L⁻¹)) analyses, the inductively coupled plasma-atomic emission spectrometer (ICP-AES, ACTIVA-M; Horiba Advanced Techno, Kisshoin, Japan) method was used. The analytical accuracy was determined using certified standards (*i.e.*, De Bruyn Spectroscopic Solutions 500 MUL20-50STD2) and recoveries were within 10 % of certified values. The metal percentage recoveries for metals ranged between 91.8 % and 106.3 %. The accuracy of the instrumental methods was checked by using a certificated reference material (River Water Reference Material for Trace Metals, NRC Canada, SLRS-4) run after every 5 samples.

2.7. Water nutrient concentration analysis

Nitrate and nitrite concentrations were determined spectrophotometrically based on the adaptation of the cadmium reduction method. This involved the reduction of NO₃⁻ to nitrite (NO₂⁻) using a copper-cadmium reduction column, before the nitrate finally reacted with sulphanilamide under acidic conditions, using N-1-naphthylethylenediamine dihydrochloride (AgrisASA, 2004). Ammonium was analysed using the spectrophotometric method based on the adaptation of ASTM manual of water and environmental technology D1426 – the Nessler method. Phosphorus (P) and phosphate (PO₄³⁻) concentration was analysed using the spectrophotometric method based on the 4500-P Phosphorus Standards Methods for Examination of Water and Wastewater as described by Rice et al. (2012).

2.8. Water quality data analysis

To assess overall river ecosystem health, we used a distance-based permutational analysis of variance (PERMANOVA) in PRIMER version 6 add-on package PERMANOVA+ based on 9999 permutations, with systems as factors (*i.e.*, Mtshabezi, Umzingwane, Inyankuni, Insiza) (Anderson and ter Braak, 2003; Anderson et al., 2008). Pairwise comparisons were conducted to assess significant differences among river systems. Furthermore, all data was assessed for normality and homogeneity of variance as was found to conform to parametric assumptions. An assessment of the differences of heavy metal and nutrient concentrations among the river systems was conducted using a one-way ANOVA analysis followed by a Tukey's post-hoc test among the significant variables. Furthermore, using a Pearson correlation, we tested for the relationships that existed between metals and nutrient concentrations. All correlations and ANOVAs were carried out in IBM SPSS Statistics version 25 (SPSS Inc, 2017).

Principal component analysis (PCA) with varimax rotation and cluster analysis (CA) using the average group linkage method was employed using the heavy metal concentrations to determine natural and anthropogenic sources of contamination. A two-way hierarchical cluster analysis (HCA) based on metal concentration data sampled across systems was carried out to identify patterns in the metal

concentrations for the different systems. The HCA was based on correlation as a distance of measure and Ward's method as the group linkage method (Sekabira et al., 2010). All multivariate analysis was carried out in PC-ORD version 5.10 (McCune and Grace, 2002).

3. Results

3.1. Land use and land cover analysis

The LULC analysis conducted in the Umzingwane River catchment unveiled seven distinct classes, each representing different types of land use within the area. These classes were categorized as artisanal mines, bare surfaces, settlements, official mines, water (including reservoirs, lakes, wetlands, and rivers), croplands, and natural vegetation, which includes trees, shrublands, and grasslands (Fig. 3). Croplands and natural vegetation dominated the landscape, covering an expansive area of 2000 ha (ha) and 5727 ha, respectively. In contrast, the least prominent land cover classes were bare surfaces and artisanal mines, covering 0.13 ha and 1.98 ha, respectively (Fig. 3). It further was observed that

artisanal mines were primarily concentrated along the riverbanks, particularly along the course of the Umzingwane River. This indicated a strong association between illegal mining activities and their proximity to water bodies (Fig. 3). On the other hand, croplands were predominantly located towards the southern regions of the catchment. Additionally, the presence of settlements, official mines, and other land use classes were also evident throughout the catchment, contributing to the overall landscape dynamics. The detailed results of the LULC analysis not only provided a comprehensive understanding of the land use patterns within the Umzingwane River catchment but also shed light on the spatial distribution of artisanal mines in relation to water bodies and agricultural activities.

3.2. The land use and land cover accuracy assessment

The assessment of the classification accuracy for the land cover classification produced satisfactory results, with an overall accuracy (OA) of 78.9 % and a Kappa coefficient of 72.8 %. These values fell within acceptable ranges, indicating the reliability of the classification

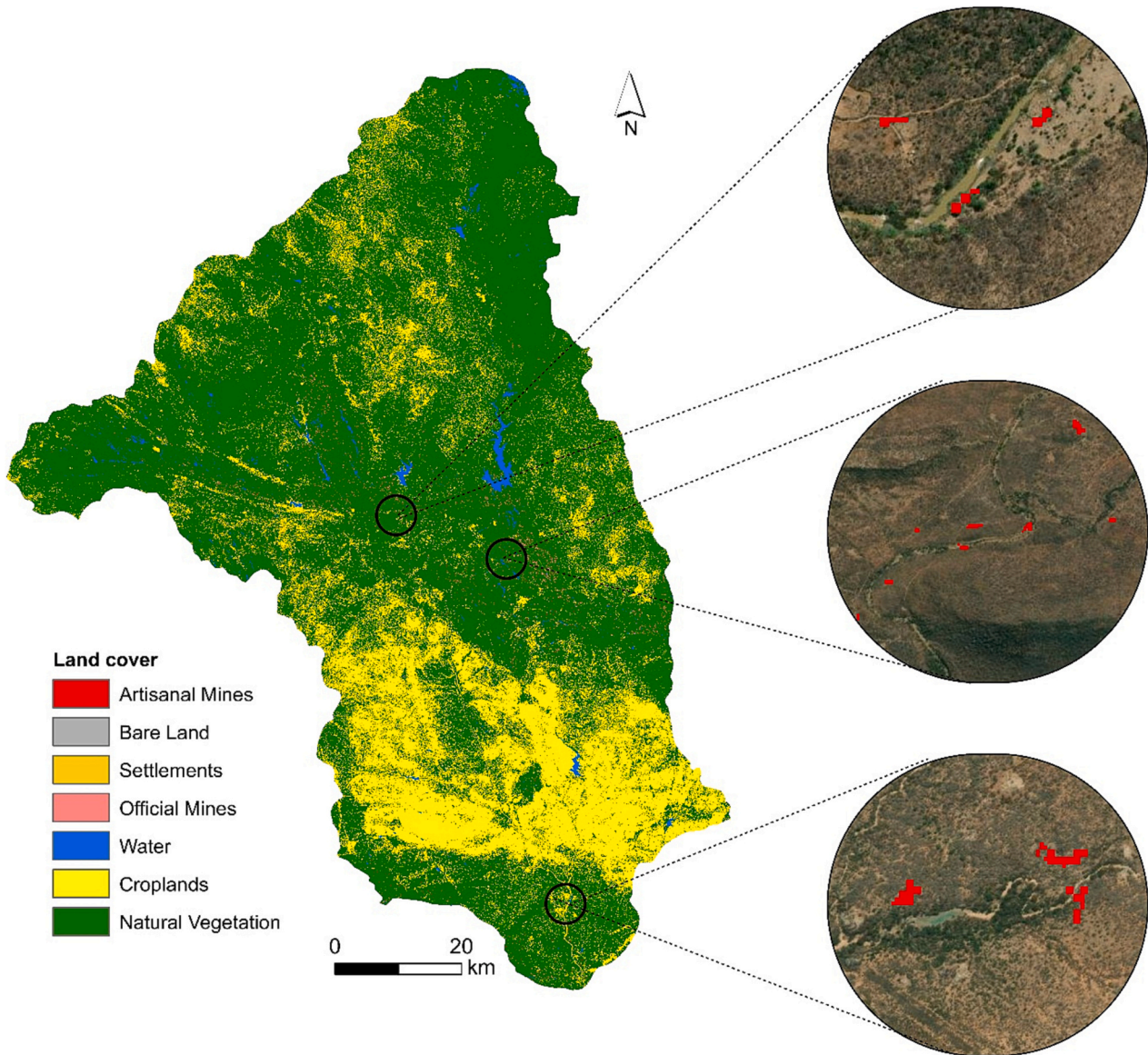


Fig. 3. Spatial distribution of various land cover types based on RF model along the Umzingwane River catchment. The zoomed inserts highlight the areas affected by artisanal mining and where field sampling was conducted. Land cover classes and their areas: artisanal mines (1.98 ha), bare surface (0.13 ha), settlements (51.44 ha), official mines (34.93 ha), water (67.95 ha), croplands (2000.17 ha) and natural vegetation (5727.64 ha).

model as per the ranges given in Gwitira et al. (2015). To further evaluate the accuracy, class accuracy results were measured using producer's accuracy (PA) and user's accuracy (UA) metrics for each land cover class.

The analysis further revealed that most land cover classes achieved acceptable accuracy levels, with PA and UA values ranging from 60 % to 100 % (Fig. 4). Notably, croplands exhibited relatively low PA and UA values, yet they still surpassed the 60 % threshold, indicating that the model was able to correctly identify them to a considerable extent. Conversely, other land cover classes, such as bare surfaces, artisanal mines, settlements, official mines, and water, demonstrated high accuracy, with PA and UA values ranging between 80 % and 100 %.

During the analysis of variable importance, several key variables played significant roles in the land cover classification. The Normalized Difference Water Index (MNDWI), Normalized Difference Vegetation Index (NDVI), and elevation emerged as the most influential variables in the classification process. These variables effectively contributed to the accurate identification and differentiation of various land cover classes. On the other hand, terrain aspects had a relatively lesser impact on the classification process (Fig. 5).

3.3. Water nutrient and metal concentrations

Mean variation in nutrient concentrations shows that nitrate (NO_3^-) and ammonium (NH_4^+) were the most dominant nutrient ranging between 0.10 mg L^{-1} to 20.0 mg L^{-1} in all the rivers except in the Inyankuni River where NO_3^- and NH_4^+ were the least dominating. Orthophosphate (PO_4^{2-}) and Phosphorus (P) were also the least dominant nutrients in all the rivers ranging from 0.03 to 0.10 mg L^{-1} (Table 2). Analysis of metals revealed that Na, Ca and Mg were the most dominant for all the rivers ranging from 10.3 to 17.1 mg L^{-1} for Na, 22.3 – 32.9 mg L^{-1} for Ca, and 5.7 – 12.1 mg L^{-1} for Mg. Low concentrations were observed for Pb, Zn, Hg, Cu, As, Cr and B with concentrations ranging from 0.001 to 2.04 mg L^{-1} for all the rivers (Table 2). Based on the ANOVA analysis, nitrates ($p = 0.034$) were found to be the only nutrients that were significantly different across systems (Table 1). Tukey's posthoc analysis indicated that Mtshabezi vs Umzingwane rivers were the only significant (ANOVA, $p = 0.025$) systems in terms of nitrate concentrations (Table 1). In terms of water metal concentrations, Na ($p = 0.005$), Mg ($p = 0.031$), As ($p = 0.001$), B ($p = 0.014$), Cu ($p = 0.014$), Pb ($p = 0.014$) and Mn ($p < 0.001$) were the only significantly different metal concentrations among systems (Table 3). Based on pairwise comparisons, Umzingwane vs Inyankuni (Na), Insiza vs Inyankuni (Mg), Mtshabezi vs Insiza (As, B, Cu, Pb, Mn), Mtshabezi vs Umzingwane (As, B, Cu, Pb, Mn) and Mtshabezi vs Inyankuni (As, B, Cu, Pb, Mn) were the significant systems for the selected metals (Table 3). From the available DWAF surface water quality guidelines, most of the parameters were above the recommended guidelines (Table 2).

The overall river ecosystem health was found to be significantly different across river systems (PERMANOVA, Pseudo-F = 1.946, p (Monte-Carlo (MC)) = 0.035). Using pairwise comparisons, we observed no significant differences for Mtshabezi vs Insiza ($t = 1.065$, p (MC) = 0.471), Mtshabezi vs Umzingwane ($t = 1.255$, p (MC) = 0.393), Mtshabezi vs Inyankuni ($t = 1.435$, p (MC) = 0.329), Insiza vs Umzingwane ($t = 1.141$, p (MC) = 0.286), Insiza vs Inyankuni ($t = 1.242$, p (MC) = 0.316) and Umzingwane vs Inyankuni ($t = 1.273$, p (MC) = 0.298).

3.4. Relationships between the measured variables

To analyse further the general water characteristics of the studied systems, we employed multivariate Pearson correlations (Table 4), cluster analysis (Fig. S1) and principal component analysis (PCA; Table 5). A correlation matrix showed that most nutrients and metals in the river water were not highly correlated with each other signifying a weak relationship (Table 4). Hence, this suggests that all metals in the studied water samples may have originated from different sources. For example, B concentrations was strongly positively correlated with Cu, Fe, Pb and Mn, while Mn strongly positively correlated with B, Cu, Fe and Pb, and Na was strongly positively correlated with Ca, Mg and P. The NO_3^- concentration was strongly positively correlated with NO_2^- , NH_4^+ , As, Fe and Mn (Table 4). Using PCA, the first two principal components (PC) explained 53.8 % of the total variance, with PC1 and PC2 explaining 31.7 % and 22.1 % of the total variance, respectively. The Eigenvalues of the two extracted PCs were both >1.0 . Principal CA classified metals into three groups, with group 1 consisting of B, Cu, Fe, Pb and Mn, group 2 – Na, K, Ca, Mg and Hg, and group 3 consisting of As, Cd, Cr and Zn (Table 5). Hierarchical cluster analysis (HCA) results

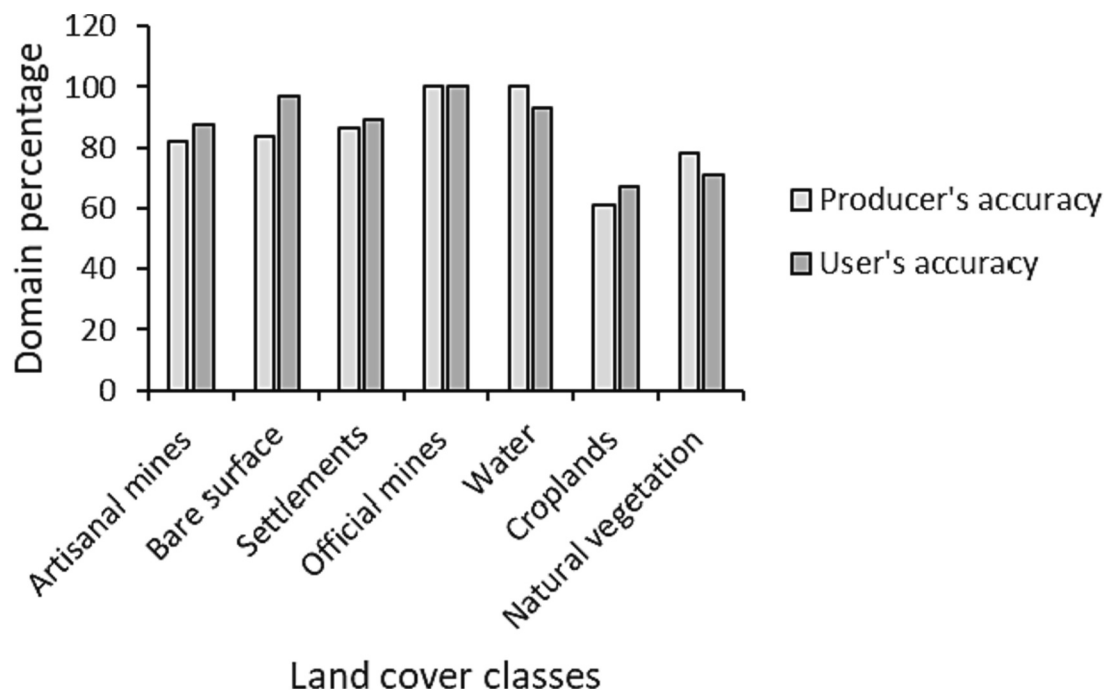


Fig. 4. The producer's accuracy and user's accuracy based on the RF model for the Umzingwane River catchment.

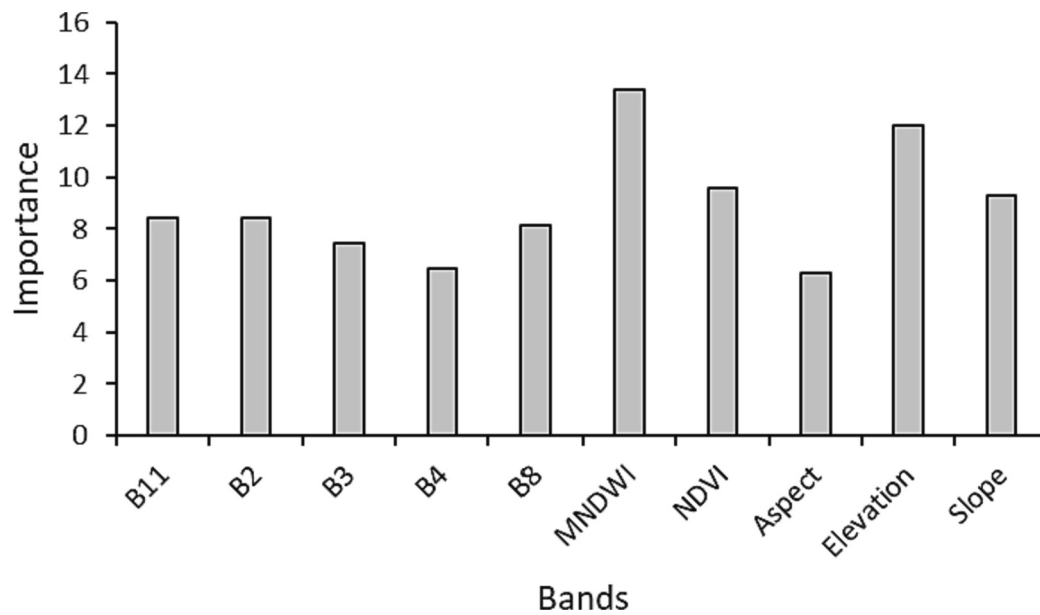


Fig. 5. Random forest variable significance based on multi-probability approach for the Umzingwane River catchment. Abbreviations: B11 – short-wave infrared, B2 – blue, B3 – green, B4 – red, B8 – near-infrared, MNDWI – modified normalized difference water index, NDVI – normalized difference water index. The B2, B3, B4 and B8 are Sentinel-2 spectral band channels with 10 m resolution and B11 is a Sentinel-2 spectral band channel with a ground sampling distance of 20 m.

Table 2

Mean variation in nutrient and metal concentration among river systems and one-way analysis of variance results. Values in bold indicate significant difference at $p < 0.05$. Abbreviation: df – degrees of freedom, DWAF – Department of Water Affairs (now Department of Water and Sanitation) surface water guidelines.

Parameter	DWAF	Mtshabezi River	Insiza River	Umzingwane River	Inyankuni River	df	F	p
Nutrients								
Nitrate (NO_3^- ; mg L^{-1})		20.0 ± 12.7	4.6 ± 11.7	0.14 ± 0.05	0.1	3	3.692	0.034
Nitrite (NO_2^- ; mg L^{-1})		0.05	0.05 ± 0.01	0.05	0.05	3	0.578	0.638
Orthophosphate (PO_4^{3-} ; mg L^{-1})		0.10	0.10	0.10	0.10	3	0.000	1.000
Ammonium (NH_4^+ ; mg L^{-1})	0.007	0.10	0.11 ± 0.04	0.10	0.10	3	0.578	0.638
Phosphorus (P; mg L^{-1})	0.025	0.04 ± 0.03	0.03 ± 0.01	0.05 ± 0.02	0.03 ± 0.01	3	2.978	0.063
Metals								
Sodium (Na; mg L^{-1})		16.0 ± 1.4	14.0 ± 1.2	17.1 ± 3.4	10.3 ± 0.6	3	6.286	0.005
Potassium (K; mg L^{-1})		2.1	2.4 ± 0.41	2.2 ± 1.0	1.6 ± 0.1	3	0.912	0.457
Calcium (Ca; mg L^{-1})		28.5 ± 3.5	23.6 ± 4.2	32.9 ± 12.1	22.3 ± 3.8	3	1.926	0.166
Magnesium (Mg; mg L^{-1})	0.18	8.0	12.1 ± 1.6	9.9 ± 4.1	5.7 ± 0.6	3	3.816	0.031
Arsenic (As; mg L^{-1})	0.01	0.06 ± 0.05	0.01 ± 0.01	<0.007	0.01 ± 0.001	3	8.674	0.001
Boron (B; mg L^{-1})		0.03 ± 0.004	0.03	0.03 ± 0.001	0.03	3	4.800	0.014
Cadmium (Cd; mg L^{-1})	0.0003	0.001	0.001	0.001	0.001	3	0.207	0.898
Total chromium (Cr; mg L^{-1})	0.012	0.03	0.03	0.03	0.03 ± 0.001	3	0.000	1.000
Copper (Cu; mg L^{-1})	0.0014	0.01 ± 0.002	0.01	0.01	0.01	3	4.800	0.014
Iron (Fe; mg L^{-1})	0.1	2.04 ± 1.73	0.63 ± 1.07	0.54 ± 0.29	0.53 ± 0.11	3	1.995	0.155
Lead (Pb; mg L^{-1})	0.0002	0.004 ± 0.004	0.001	0.001	0.001	3	4.800	0.014
Manganese (Mn; mg L^{-1})	0.18	0.46 ± 0.18	0.09 ± 0.08	0.13 ± 0.05	0.10 ± 0.08	3	11.379	<0.001
Mercury (Hg; mg L^{-1})	0.0004	0.001	0.001 ± 0.001	0.001	0.001	3	0.209	0.889
Zinc (Zn; mg L^{-1})	0.002	0.03	0.03	0.03	0.03	3	0.000	1.000

identified 3 distinct groups: *group 1* included Na, Ca and Mg, and was clearly distinguishable from other 2 groups (Fig. S1). *Group 2* consisted of K, As, Cr, Cd, Hg and Zn, and *group 3* had B, Cu, Pb, Mn and Fe (Fig. S1). Variability in the metal concentrations can be inferred to be controlled by the anthropogenic point sources and local bedrock materials. For the river systems two groups were identified, with *group 1* consisting of Insiza River sites and *group 2* of all the other river sites (Fig. S1).

4. Discussion

The results of the land use and land cover (LULC) analysis revealed that artisanal mines were predominantly situated along the rivers, which aligns with previous studies (Dalu et al., 2017a, 2017b, 2022)

that have observed a preference for riparian zones due to the significant water requirements of these mining operations. Mhangara et al. (2020) in Johannesburg, South Africa showed that these illegal mining systems are usually located along the surface water systems due to their large water requirements. These findings corroborate with the findings of our study. Furthermore, Nyamekye et al. (2021) using unmanned vehicle machines and random forest machine learning algorithms highlighted that small scale illegal mines were mostly found along the large surface water bodies, therefore also corroborating with the findings of our study.

Further analysis of LULC changes indicated that croplands and natural vegetation were the most dominant land cover domains, while bare surface and artisanal mines were the least dominant classes. The dominance of croplands and natural vegetation was expected as (Maviza

Table 3Tukey's pairwise comparisons among the different study systems. Values in bold indicate significant differences at $p < 0.05$.

Parameter	System pairs	<i>p</i>	Parameter	System pairs	<i>p</i>
Nitrate (NO ₃)	Msthabezi vs Insiza	0.1050	Boron (B)	Msthabezi vs Insiza	0.013
	Msthabezi vs Umzingwane	0.0250		Msthabezi vs Umzingwane	0.012
	Msthabezi vs Inyankuni	0.0570		Msthabezi vs Inyankuni	0.032
	Insiza vs Umzingwane	0.6990		Insiza vs Umzingwane	1.000
	Insiza vs Inyankuni	0.8410		Insiza vs Inyankuni	1.000
Sodium (Na)	Umzingwane vs Inyankuni	1.0000	Umzingwane vs Inyankuni	1.000	
	Msthabezi vs Insiza	0.7340	Copper (Cu)	Msthabezi vs Insiza	0.013
	Msthabezi vs Umzingwane	0.9340		Msthabezi vs Umzingwane	0.012
	Msthabezi vs Inyankuni	0.0870		Msthabezi vs Inyankuni	0.032
	Insiza vs Umzingwane	0.0990		Insiza vs Umzingwane	1.000
Insiza vs Inyankuni	0.1660	Insiza vs Inyankuni		1.000	
Magnesium (Mg)	Umzingwane vs Inyankuni	0.0040	Umzingwane vs Inyankuni	1.000	
	Msthabezi vs Insiza	0.3170	Lead (Pb)	Msthabezi vs Insiza	0.013
	Msthabezi vs Umzingwane	0.8450		Msthabezi vs Umzingwane	0.012
	Msthabezi vs Inyankuni	0.8140		Msthabezi vs Inyankuni	0.032
	Insiza vs Umzingwane	0.4540		Insiza vs Umzingwane	1.000
Insiza vs Inyankuni	0.0240	Insiza vs Inyankuni		1.000	
Arsenic (As)	Umzingwane vs Inyankuni	0.1810	Umzingwane vs Inyankuni	1.000	
	Msthabezi vs Insiza	0.0040	Manganese (Mn)	Msthabezi vs Insiza	<0.001
	Insiza vs inyankuni	583.0000		Msthabezi vs Umzingwane	<0.001
	Msthabezi vs Inyankuni	0.0030		Msthabezi vs Inyankuni	0.001
		Insiza vs Umzingwane		0.835	
			Insiza vs Inyankuni	0.997	
			Umzingwane vs Inyankuni	0.971	

and Ahmed, 2020) in the Umzingwane River catchment, reported that croplands and natural vegetation were among the most dominant for the area and with a future growth prediction of 10.7 %. Bare surface was however expected to be among the least dominating class based on the previous estimates (Maviza and Ahmed, 2020), however, bare surface was one of the most dominant land cover types during the current study period. It was further observed that there was spectral mixing between the bare lands and other land cover classes, particularly official and artisanal mines. The spectral mixing mostly caused by the spatial resolution of the remotely sensed data used In this study, which created spectral confusions between various classes which are known to have similar spectral characteristics, particularly bare surface, and exposed mining fields (both artisanal and official mining). This mixing resulted in some of the bare surface points being misclassified as official and artisanal mines. This outcome was anticipated due to the typical characteristics of mining environments, where vegetation is cleared and the soil is exposed, leading to similar spectral reflectance properties between bare surface and mining areas, particularly from the optical remote sensing data such as Sentinel-2 used in this study. Li et al. (2022) highlighted that spectral library for mines had similar spectral reflectance values with bare surfaces, and this corroborates with the findings of the current study. A similar study by Snapir et al. (2017) highlighted spectral confusions between mine boundaries other land cover types such as bare soils, and these were attributed to the spatial resolution of the remotely sensed data used. Similarly, Lobo et al. (2018) also reported spectral confusions between bare surface and open mined environments, with the confusions being attributed to the spatial resolution of the Sentinel-2 data used. Although this was the case, the use of terrain parameters such as slope, elevation and aspects as well as contextual parameters and indices proved to be useful parameters in this context, as such, the study managed to obtain acceptable class accuracies (>60 %).

Nutrient concentrations in water showed that nitrate were among the most dominant elements across various streams within the Umzingwane River catchment, particularly for the Mtshabezi River sites 1 and 2, and Inyankuni River site 1 where some nutrient concentrations were > 10 mg L⁻¹. The high nitrite and nitrate concentrations are usually associated with anthropogenic activities like agriculture and wastewater effluents discharged into the river. In this study, the elevated nitrate concentration could be attributed to mostly the dominating croplands in the region, were runoff from these regions transport nutrients from the application of fertilisers in fields to nearby streams and

rivers therefore resulting in the elevated nitrate concentrations in those rivers (Nhiwatiwa et al., 2017; Xia et al., 2020), particularly because the sampling sites Mtshabezi River sites 1 and 2 which were located in areas dominated by croplands. This was also reported in a study by Liang et al. (2022) in the Yangtze River Basin in China. Another study by Xu et al. (2021) in the Yuntaishan River in China reported elevated nitrate concentrations, and these were attributed to the agricultural runoff. In addition, high nitrate concentrations observed could have been caused by the illegal mines particularly if gold is the mineral being mined. Gold mining involves the use of ammonium nitrate-based explosives and cyanide to leach out gold which gets released with the untreated effluent from the cleaning of the ore (Logsdon et al., 1999).

In illegal mining, the effluent from the cleaning of the ore is not treated and it gets discharged to the nearby streams and rivers thus contributing to the elevated nitrate concentrations in these rivers, especially in the case of Umzingwane River, where these mines are located in the riparian zones of these selected rivers. A study by Frandsen et al. (2009), reported elevated ammonium nitrate concentration around mines, with such elevated concentrations being attributed to gold mining explosives where the effluent from the ore containing ammonium nitrates was discharged into the nearby aquatic systems. Therefore, these results by Frandsen et al. (2009) further corroborated our findings. Another study by Häyrynen et al. (2009) reported elevated nitrate concentration levels from mine effluent in Brazil. These findings also support our argument that elevated nitrate concentrations in the selected sites might also be from the artisanal mines in the riparian zones.

Metal analysis results indicated elevated concentrations of Ca, Na and Mg in most sampling sites >10 mg L⁻¹ and this was expected because of the underlying geology for the region. The lower part of the catchment is characterised by Limpopo belt gneisses and Karroo Basalt, and basaltic rocks usually contains plagioclase feldspar which is calcium rich. The excavation during mining and dewatering result in the release of water that has interacted with the Karroo basalt rock, which is Ca rich, thus leading to the high Ca concentrations since the mining effluent realised is not treated (Vazquez-Almazan et al., 2012). A study by Liu and Ma (2019), reported high Ca concentrations in a river in China from the dewatering that has interacted with a Ca rich mineral, thus corroborating with the findings of our study. The high Mg and Na concentrations observed in some of the sampling sites was expected, particularly for the sampling points located in the upper catchment due

Table 4 Pearson correlation among the nutrient and metal concentrations among the different systems. Abbreviations: ** – Correlation is significant at the $p < 0.01$ level, * – Correlation is significant at the $p < 0.05$ level. Bold values indicate significant correlation differences.

	NO ₃ ⁻	NO ₂ ⁻	PO ₄	NH ₄ ⁺	Na	K	Ca	Mg	As	B	Cd	Cr	Cu	Fe	Pb	Mn	Hg	P	Zn
NO ₃ ⁻	1.00	0.69 ^{**}	0.12	0.69 ^{**}	-0.01	-0.05	-0.02	0.04	0.66 ^{**}	0.19	-0.13	0.12	0.19	0.65 ^{**}	0.20	0.47 [*]	0.44	-0.21	0.12
NO ₂ ⁻		1.00	0.08	1.00 ^{**}	-0.07	-0.03	-0.02	0.21	0.01	-0.05	-0.08	0.08	-0.05	0.62 ^{**}	-0.03	0.04	0.69 ^{**}	-0.16	0.08
PO ₄			1.00	0.08	-0.32	0.21	-0.35	-0.41	0.14	0.08	0.11	0.44 [*]	0.08	0.06	0.08	-0.20	0.11	-0.14	0.44 [*]
NH ₄ ⁺				1.00	-0.07	-0.03	-0.02	0.21	0.01	-0.05	-0.08	0.08	-0.05	0.62 ^{**}	-0.03	0.04	0.69 ^{**}	-0.16	0.08
Na					1.00	-0.35	0.87 ^{**}	0.67 ^{**}	-0.07	0.15	0.17	-0.43	0.15	-0.01	0.16	0.27	0.17	0.51 [*]	0.04
K						1.00	-0.64 ^{**}	-0.42	0.04	-0.03	0.01	0.19	-0.03	0.06	-0.04	-0.17	-0.21	0.06	-0.22
Ca							1.00	0.62 ^{**}	-0.11	0.09	0.26	-0.31	0.09	-0.02	0.10	0.27	0.26	0.43	0.15
Mg								1.00	-0.10	-0.13	0.26	-0.46 [*]	0.16	-0.14	-0.12	-0.04	0.31	0.01	-0.02
As									1.00	0.16	-0.13	0.16	0.16	0.19	0.16	0.45 [*]	-0.06	-0.15	0.17
B										1.00	-0.08	0.08	1.00 ^{**}	0.69 ^{**}	1.00 ^{**}	0.79 ^{**}	-0.08	0.25	0.076
Cd											1.00	1.00	-0.08	-0.21	-0.06	-0.17	0.44 [*]	-0.18	0.44 [*]
Cr												1.00	1.00	0.08	0.08	-0.06	0.11	-0.38	0.44 [*]
Cu													1.00	0.69 ^{**}	1.00 ^{**}	0.79 ^{**}	-0.08	0.25	0.08
Fe														1.00	0.70 ^{**}	0.70 ^{**}	0.37	0.16	-0.05
Pb															1.00	0.79 ^{**}	-0.05	0.25	0.08
Mn																1.00	0.01	0.32	-0.10
Hg																	1.00	-0.14	0.11
P																		1.00	-0.24
Zn																			1.00

Table 5

Principle component analysis (PCA) results for metal concentrations for the entire study area. Factor loadings >0.5 are highlighted in bold.

Factors	PC 1	PC 2
Eigenvalue	4.435	3.091
% of variance	31.679	22.081
Cum. % of variance	31.679	53.76
Metals		
Factor loadings		
Sodium (Na)	0.23	-0.84
Potassium (K)	-0.12	0.66
Calcium (Ca)	0.2	-0.90
Magnesium (Mg)	-0.06	-0.84
Arsenic (As)	0.29	0.16
Boron (B)	0.96	0.10
Cadmium (Cd)	-0.08	0.00
Total Chromium (Cr)	0.12	-0.13
Copper (Cu)	0.96	0.10
Iron (Fe)	0.78	0.20
Lead (Pb)	0.96	0.10
Manganese (Mn)	0.91	-0.10
Mercury (Hg)	-0.01	-0.51
Zinc (Zn)	0.08	0.23

to the greenstone belt geology underlain by the granitic terrains. Greenstone belt consist of sill-like plutonic ultramafic-mafic rocks that are genetically related to high-Mg magmas like komatiites, boninites, and high-Mg siliceous basalts. Thus, the dissolution of these rocks results in the release of Mg (Ashton et al., 2001; Munyai et al., 2023). Similar to Ca, the dewatering during the mining process could have resulted in the release of Mg rich water into the studied rivers.

The results of the Pearson correlation matrix analysis provided important insights into the relationship between nutrient and metal concentrations in the river waters. The significant relationships observed indicate that changes in these concentrations can be attributed to various anthropogenic activities occurring in the area. In particular, the presence of illegal mines in the riparian zones of the rivers appears to have a significant impact on water quality. The proximity of the mines to the rivers and their associated riparian zones facilitates the direct entry of contaminants into the water, potentially leading to increased levels of nutrients and metals (Dube et al., 2023). The Principal Component Analysis and hierarchical cluster analysis revealed the presence of three distinct groups with significant variations (>50 %) between the clusters. The first cluster comprised Na, Mg, and Ca, which are associated with the hardness of water caused by mineral gypsum and probable come from illegal mining areas and this finding probable indicates the influence of mining activities, particularly the artisanal mines located in the riparian zones. In areas dominated by artisanal mining activities, the presence of mercury in water bodies poses a significant concern for water quality. Artisanal and small-scale gold mining commonly involves the use of mercury as a means of extracting gold from ore. As a result, water sources in these areas can become contaminated with mercury. This process releases mercury into the environment, leading to widespread pollution of water sources due to widespread use of mercury to extract gold by the illegal miners (Thandekile Dube, pers. Observ.). These might results highlight the complex interactions between different sources of water pollution within the study area as most parameters were above the surface water guidelines and the PCA analysis highlighted potential different sources of origin for the metals.

The study findings indicate that the presence of artisanal mines, along with other land cover types, along Umzingwane River catchment have an impact on river water quality as the water contaminated with different metals and they made the river to be very turbid, with high sediment load. These findings provide a valuable baseline understanding of the overall river health and the influence of surrounding anthropogenic activities in the area. It is therefore crucial to use this information in the development and implementation of regulatory

measures to protect and preserve our aquatic systems, as well as strengthen existing regulations. The mitigation of mercury pollution resulting from artisanal mining activities is crucial for achieving the Sustainable Development Goals (SDGs), particularly SDG 15.1, which focuses on the protection, restoration, and conservation of terrestrial and inland freshwater systems and their ecosystem services (Arora and Mishra, 2019). Artisanal and small-scale gold mining has been recognised as a significant source of mercury contamination in water bodies (Cordy et al., 2011; Telmer and Veiga, 2009). Mercury is used in the amalgamation process to extract gold from ore, leading to environmental contamination and posing risks to human health (Veiga and Baker, 2004; García et al., 2015). Furthermore, the findings of this research directly align with SDG 3.9, which aims to reduce water-related deaths caused by water contamination (United Nations, 2015). Mercury-contaminated water can have severe health impacts, including neurological disorders, developmental issues, and organ damage (Bose-O'Reilly et al., 2010; Esdaile and Chalker, 2018). Minimising the use of mercury in artisanal mining and implementing proper waste management practices are crucial steps in reducing water contamination and associated health risks (Bose-O'Reilly et al., 2010; Hilson and McQuilken, 2014).

Therefore, implementing strategies such as promoting mercury-free gold processing techniques, providing training and support to artisanal miners, and strengthening regulatory frameworks are essential for addressing the challenges posed by mercury pollution in artisanal mining areas (Hilson and McQuilken, 2014; García et al., 2015). Collaborative efforts involving governments, mining communities, non-governmental organizations, and international institutions are necessary to achieve sustainable mining practices and contribute to the attainment of the SDGs.

4.1. Policy implications of the study

The findings of this study have significant policy implications that align with several sustainable development goals (SDGs). The findings highlight the need for stringent regulations and policy frameworks to control artisanal mining activities along rivers and riparian zones, as well as promoting sustainable agricultural practices, contribute to SDG 6 (clean water and sanitation) through the safeguarding of water quality and preserving aquatic ecosystems. Additionally, promoting sustainable agricultural practices can help reduce nutrient runoff from croplands, while policy measures to minimise Hg use in artisanal mining and enforce proper waste management can prevent widespread contamination of aquatic ecosystems and safeguard human health. The study has significant policy implications that call for stringent regulations to control artisanal mining operations situated along unprotected rivers and riparian zones. Furthermore, designating protected areas along river ecosystems aligns with SDG 14 (life below water) and SDG 15 (life on land) as it preserves sensitive aquatic ecosystems and contributes to biodiversity conservation. There is a need for the establishment of robust monitoring systems and collaborative governance efforts involving multi-stakeholder cooperation and knowledge exchange for effective water resource management. Also, public awareness campaigns and educational programs addressed by SDG 4 on promoting responsible water use and environmental awareness is therefore crucial. By integrating policy implications into decision-making processes, policymakers can actively work towards achieving various SDGs, ensuring the sustainable management of water resources, protecting ecosystems, and promoting overall sustainable development.

5. Conclusions

The analysis of LULC in the studied area identified seven distinct classes, including artisanal mines, with an acceptable overall accuracy. This suggests that the classification approach successfully captured the different land cover types present in the Umzingwane River catchment.

Interestingly, the study found that artisanal mines were predominantly located along the riparian zones of the rivers, which can be attributed to their significant water requirements for mining operations. Water quality analysis revealed elevated concentrations of nitrate and nitrite in the rivers, which can be linked to the presence of croplands and potential artisanal mining activities in the area. The use of fertilisers in agriculture contributes to the increased nitrate and nitrite levels, while the mining activities, including the use of ammonium nitrate explosives, contribute to the elevated ammonium concentrations. These mining-related activities release ammonium into the river systems as untreated effluents, further impacting water quality. These findings provide valuable insights into the health status of the rivers in the Umzingwane River catchment and the impacts of anthropogenic activities, particularly artisanal mining and agriculture. By understanding the spatial distribution of land cover classes, including the location of artisanal mines, and identifying the associated water quality variations, policy-makers and environmental managers can make informed decisions to mitigate the negative impacts on river ecosystems.

Supplementary data to this article can be found online at <https://doi.org/10.1016/j.scitotenv.2023.167919>.

CRediT authorship contribution statement

Thandekile Dube: writing of the manuscript and data collection, **Siyamthanda Gxokwe:** writing of the manuscript and data analysis, **Timothy Dube:** funding, conceptualization, writing, reviewing and editing, **Tatenda Dalu:** funding, conceptualization, data analysis, writing, reviewing and editing, **Thomas Marambanyika:** reviewing and editing. All the authors have read and agree to the final submission of this paper.

Funding

The funding for this project is provided by the Global Monitoring for Environment and Security and Africa GMES–Africa, which played a crucial role in the successful implementation of the SASSCAL–WeMAST Phase II Project and WRC Project (grant no. C2022/2023–00902). Tatenda Dalu expresses gratitude for the financial support received from the National Research Foundation (grant no. 138206).

Declaration of competing interest

The authors declare that there are no known competing interests whether funding nor data related.

Data availability

Data will be made available on request.

Acknowledgments

The authors express their gratitude to the anonymous reviewers for their valuable feedback and contributions to improving the manuscript. We extend our appreciation to the Global Monitoring for Environment and Security and Africa (GMES and Africa) for their financial support, which was instrumental in the successful completion of the SASSCAL–WeMAST Phase II Project. The authors would also like to acknowledge the Environmental Management Agency – Zimbabwe for their logistical support and valuable input to the study.

References

- Achanta, R., Süsstrunk, S., 2017. Superpixels and polygons using simple non-iterative clustering. In: *Proceedings – 30th IEEE Conference on Computer Vision and Pattern Recognition, CVPR 2017*, pp. 4895–4904.
- Agriculture Laboratory Association of Southern Africa (AgriLASA), 2004. *Soil handbook*. Agriculture Laboratory Association of Southern Africa, Pretoria.

- Amuah, E.E.Y., Fei-Baffoe, B., Kazapoe, R.W., 2021. Emerging potentially toxic elements (strontium and vanadium) in Ghana's pedological studies: understanding the levels, distributions and potential health implications. A preliminary review. *Environ. Chall.* 5, 100235.
- Anderson, M.J., ter Braak, C.J.F., 2003. Permutation tests for multi-factorial analysis of variance. *J. Stat. Comput. Simul.* 73, 85–113.
- Anderson, M.J., Gorley, R.N., Clarke, K.R., 2008. PERMANOVA+ for PRIMER: Guide to Software and Statistical Methods. PRIMER-E, Plymouth, UK.
- Arora, N.K., Mishra, I., 2019. United Nations Sustainable Development Goals 2030 and environmental sustainability: race against time. *Environ. Sustain.* 2 (4), 339–342.
- Ashton, P., Love, D., Mahachi, H., Dirks, P., 2001. An overview of the impact of mining and mineral processing operations on water resources and water quality in the Zambezi, Limpopo and Olifants catchments in southern Africa resources and water quality in the Zambezi. In: Contract Report to the Mining, Minerals and Sustainable Development (Southern Africa) Project, by CSIR–Environmentek, Pretoria and Geology Department, University of Zimbabwe, Harare. Report No. ENV-PC, 42, pp. 1–362.
- Bose-O'Reilly, S., McCarty, K.M., Steckling, N., Lettmeier, B., 2010. Mercury exposure and children's health. *Curr. Probl. Pediatr. Adolesc. Health Care* 40 (8), 186–215.
- Chisadzwa, B., Ncube, F., Macherera, M., Bangira, T., Gwate, O., 2023. Spatio-temporal variations in the ecological vulnerability of the Upper Mzingwane sub-catchment of Zimbabwe. *Geomat. Nat. Haz. Risk* 14. <https://doi.org/10.1080/19475705.2023.2190857>.
- Cordy, P., Veiga, M.M., Salih, I., Al-Saadi, S., Console, S., Garcia, O., Mesa, L.A., Velázquez-López, P.C., Roeser, M., 2011. Mercury contamination from artisanal gold mining in Antioquia, Colombia: the world's highest per capita mercury pollution. *Sci. Total Environ.* 410, 154–160.
- Dalu, M.T.B., Wasserman, R.J., Dalu, T., 2017a. A call to halt destructive, illegal mining in Zimbabwe. *S. Afr. J. Sci.* 113, 11–12.
- Dalu, T., Wasserman, R.J., Tonkin, J.D., Alexander, M.E., Dalu, M.T.B., Motitsoe, S.N., Manungo, K.I., Bepe, O., Dube, T., 2017b. Assessing drivers of benthic macroinvertebrate community structure in African highland streams: an exploration using multivariate analysis. *Sci. Total Environ.* 601–602, 1340–1348.
- Dalu, T., Wasserman, R.J., Wu, Q., Froneman, W.P., Weyl, O.L.F., 2018. River sediment metal and nutrient variations along an urban–agriculture gradient in an arid austral landscape: implications for environmental health. *Environ. Sci. Pollut. Res.* 25 (3), 2842–2852.
- Dalu, T., Banda, T., Mutshekwa, T., Munyai, L.F., Cuthbert, R.N., 2021. Effects of urbanisation and a wastewater treatment plant on microplastic densities along a subtropical river system. *Environ. Sci. Pollut. Res.* 28, 36102–36111.
- Dalu, T., Mwedzi, T., Wasserman, R.J., Madzivanzira, T.C., Nihwatiwa, T., Cuthbert, R.N., 2022. Land use effects on water quality, habitat, and macroinvertebrate and diatom communities in African highland streams. *Sci. Total Environ.* 846, 157346.
- Dube, T., Dube, T., Marambanika, T., 2023. A review of wetland vulnerability assessment and monitoring in semi-arid environments of sub-Saharan Africa. *Phys. Chem. Earth, Parts A/B/C* 132, 103473.
- Duncan, A.E., 2020. The dangerous couple: illegal mining and water pollution – a case study in Fena River in the Ashanti Region of Ghana. *J. Chem.* 2020 <https://doi.org/10.1155/2020/2378560>.
- Dzurume, T., Dube, T., Thamaga, K.H., Shoko, C., Mazvimavi, D., 2021. Use of multispectral satellite data to assess impacts of land management practices on wetlands in the Limpopo Transfrontier River Basin. *South Africa. South Afr. Geogr. J.* 00, 1–20.
- Ericsson, M., Löf, O., 2019. Mining's contribution to national economies between 1996 and 2016. *Miner. Econ.* 223–250.
- Esdaile, L.J., Chalker, J.M., 2018. The mercury problem in artisanal and small-scale gold mining. *Chem. Eur. J.* 24 (27), 6905–6916.
- Frandsen, S., Widerlund, A., Herbert, R., Öhlander, B., 2009. Nitrogen effluents from mine sites in northern Sweden: environmental effects and removal of nitrogen in recipients. In: Presented at the Securing the Future and 8th ICARD Conference. Skellefteå, Sweden. 23–26 June 2009.
- García, O., Veiga, M.M., Cordy, P., Suescún, O.E., Molina, J.M., Roeser, M., 2015. Artisanal gold mining in Antioquia, Colombia: a successful case of mercury reduction. *J. Clean. Prod.* 90, 244–252.
- Gwitira, I., Murwira, A., Zengeya, F.M., Masocha, M., Mutambu, S., 2015. Modelled habitat suitability of a malaria causing vector (*Anopheles arabiensis*) relates well with human malaria incidences in Zimbabwe. *Appl. Geogr.* 60, 130–138.
- Gxokwe, S., Dube, T., Mazvimavi, D., 2021. Leveraging Google Earth Engine platform to characterize and map small seasonal wetlands in the semi-arid environments of South Africa. *Sci. Total Environ.* 803, 150139.
- Gxokwe, S., Dube, T., Mazvimavi, D., Grenfell, M., 2022. Using cloud computing techniques to monitor long-term variations in ecohydrological dynamics of small seasonally-flooded wetlands in semi-arid South Africa. *J. Hydrol.* 612, 128080.
- Häyrynen, K., Pongrácz, E., Väisänen, V., Pap, N., Mänttari, M., Langwaldt, J., Keiski, R. L., 2009. Concentration of ammonium and nitrate from mine water by reverse osmosis and nanofiltration. *Desalination* 240, 280–289.
- Hilson, G., McQuilken, J., 2014. Four decades of support for artisanal and small-scale mining in sub-Saharan Africa: a critical review. *Extr. Ind. Soc.* 1 (1), 104–118.
- Hodge, R.A., Ericsson, M., Löf, O., Löf, A., Semkowich, P., 2022. The global mining industry: corporate profile, complexity, and change. *Miner. Econ.* 35, 587–606.
- Kessey, K.D., Arko, B., 2013. Small scale gold mining and environmental degradation, in Ghana : issues of mining policy implementation and challenges introduction Ghana has a long history of small scale gold mining, but at the peak of colonial exploration ; Europeans introduced larg. *J. Stud. Soc. Sci.* 5, 12–30.
- Laxen, D.P., Harrison, R.M., 1981. Cleaning methods for polythene containers prior to the determination of trace metals in fresh water samples. *Anal. Chem.* 53 (2), 345–350.
- Li, X., Zhou, T., Li, Z., Wang, W., Zhou, J., Hu, P., Luo, Y., Christie, P., Wu, L., 2022. Legacy of contamination with metal (loid) s and their potential mobilization in soils at a carbonate-hosted lead-zinc mine area. *Chemosphere* 308, 136589.
- Liang, Y., Ma, R., Nghiem, A., Xu, J., Tang, L., Wei, W., Prommer, H., Gan, Y., 2022. Sources of ammonium enriched in groundwater in the central Yangtze River Basin: anthropogenic or geogenic? *Environ. Pollut.* 306, 119463.
- Liu, S., Ma, W., 2019. Calcium-bearing minerals transformation during underground coal gasification. *Minerals* 9. <https://doi.org/10.3390/min9110708>.
- Lobo, F. de L., Souza-Filho, P.W.M., Novo, E.M.L. de M., Carlos, F.M., Barbosa, C.C.F., 2018. Mapping mining areas in the Brazilian amazon using MSI/Sentinel-2 imagery (2017). *Remote Sens.* 10 <https://doi.org/10.3390/rs10081178>.
- Logsdon, M.J., Hagelstein, K., Mudder, T., 1999. The Management of Cyanide in Gold Extraction. International Council on Metals and the Environment, Ottawa.
- Mapaure, I., McCartney, M.P., 2001. Vegetation–environment relationships in a catchment containing a dambo in Central Zimbabwe. *Bothalia* 31 (135–143), 1.
- Maviza, A., Ahmed, F., 2020. Analysis of past and future multi-temporal land use and land cover changes in the semi-arid Upper-Mzingwane sub-catchment in the Matabeleland south province of Zimbabwe. *Int. J. Remote Sens.* 41, 5206–5227.
- McCune, B., Grace, J.B., 2002. Analysis of Ecological Communities. MjM Software, Glenden Beach, OR, USA.
- McFeeters, S.K., 1996. The use of the Normalized Difference Water Index (NDWI) in the delineation of open water features. *Int. J. Remote Sens.* 17, 1425–1432.
- Mhangara, P., Tsoeleng, L.T., Mapurisa, W., 2020. Monitoring the development of artisanal mines in South Africa. *J. South. Afr. Inst. Min. Metall.* 120 (4), 299–306.
- Mtengwana, B., Dube, T., Mkunyanana, Y.P., Mazvimavi, D., 2020. Use of multispectral satellite datasets to improve ecological understanding of the distribution of invasive alien plants in a water-limited catchment, South Africa. *Afr. J. Ecol.* <https://doi.org/10.1111/aje.12751>.
- Munyai, L.F., Mugwedi, L., Wasserman, R.J., Dondofema, F., Riddell, E., Keates, C., Dalu, T., 2023. Metal and non-metal dynamics and distribution in soil profiles across selected pans in the Ramsar declared subtropical within national protected area. *Chem. Ecol.* <https://doi.org/10.1080/02757540.2023.2269140>.
- Nasirudeen, A.F., Allan, A., 2014. Managing the impacts of mining on Ghana's water resources from a legal perspective. *J. Energy Nat. Resour. Manag.* 1 (3), 156–165.
- Nihwatiwa, T., Dalu, T., Brendonck, L., 2017. Impact of irrigation based sugarcane cultivation on the Chiredzi and Runde Rivers quality, Zimbabwe. *Sci. Total Environ.* 587, 316–325.
- Nyamekye, C., Ghansah, B., Agyapong, E., Kwofie, S., 2021. Mapping changes in artisanal and small-scale mining (asm) landscape using machine and deep learning algorithms—a proxy evaluation of the 2017 ban on asm in Ghana. *Environ. Chall.* 3, 100053.
- Omotehinse, A.O., De Tomi, G., 2023. Mining and the sustainable development goals: prioritizing SDG targets for proper environmental governance. *Ambio* 52, 229–241.
- Owusu-Boateng, G., Kumi-Aboagye, E., 2013. An assessment of the status of pollution of the Lake Amponsah in the Faculty of Renewable and Natural Resources, Kwame Nkrumah University of Science and Technology. *Kumasi. Am. J. Sci. Ind. Res.* 4, 499–511.
- Quarm, J.A., Anning, A.K., Fei-Baffoe, B., Siaw, V.F., Amuah, E.E.Y., 2022. Perception of the environmental, socio-economic and health impacts of artisanal gold mining in the Amansie West District. *Ghana. Environ. Chall.* 9, 100653.
- Rice, E.W., Bridgewater, L., Association, A.P.H., 2012. Standard Methods for the Examination of Water and Wastewater. American Public Health Association, Washington, DC.
- Seccatore, J., Veiga, M., Origliasso, C., Marin, T., De Tomi, G., 2014. An estimation of the artisanal small-scale production of gold in the world. *Sci. Total Environ.* 496, 662–667.
- Sekabira, K., Origa, H.O., Basamba, T.A., Mutumba, G., Kakudidi, E., 2010. Assessment of heavy metal pollution in the urban stream sediments and its tributaries. *Int. J. Environ. Sci. Technol.* 7, 435–446.
- Sibandza, S., Grab, S.W., Ahmed, F., 2020. Long-term rainfall characteristics in the Mzingwane catchment of South-Western Zimbabwe. *Theor. Appl. Climatol.* 139, 935–948.
- Simioni, J.P.D., Guasselli, L.A., de Oliveira, G.G., Ruiz, L.F.C., de Oliveira, G., 2020. A comparison of data mining techniques and multi-sensor analysis for inland marshes delineation. *Wetl. Ecol. Manag.* 28, 577–594.
- Snapir, B., Simms, D.M., Waine, T.W., 2017. Mapping the expansion of galamsey gold mines in the cocoa growing area of Ghana using optical remote sensing. *Int. J. Appl. Earth Obs. Geoinf.* 58, 225–233.
- SPSS Inc., 2017. SPSS Release 16.0.0 for Windows. In: Polar Engineering and Consulting. SPSS Inc., Chicago.
- Stoudmann, N., García, C., Randriamalala, I.H., Rakotomalala, V.A., Ramamonjisoa, B., 2016. Two sides to every coin: farmers' perceptions of mining in the Maningory watershed. *Madagascar. Madagascar Conserv. Dev.* 11, 91.
- Telmer, K.H., Veiga, M.M., 2009. World emissions of mercury from artisanal and small scale gold mining. In: Mason, R., Pirrone, N. (Eds.), *Mercury Fate and Transport in the Global Atmosphere: Emissions, Measurements and Models*. Springer-Verlag US, Boston, MA.
- Thamaga, K.H., Dube, T., Shoko, C., 2022. Evaluating the impact of land use and land cover change on unprotected wetland ecosystems in the arid-tropical areas of South Africa using the Landsat dataset and support vector machine. *Geocarto Int.* 0, 1–22.
- Vazquez-Almazan, M.C., Ventura, E., Rico, E., Rodríguez-García, M.E., 2012. Use of calcium sulphate dihydrate as an alternative to the conventional use of aluminium sulphate in the primary treatment of wastewater. *Water SA* 38 (5), 813–818.

- Veiga, M.M., Baker, R., 2004. Protocols For Environmental and Health Assessment of Mercury Released By Artisanal and Small-Scale Gold Miners. Pub. GEF/UNDP/UNIDO Global Mercury Project, Vienna, p. 289. Available at. <https://iwlearn.net/retrieve/617e8a7184a7ec1e292a61c2319dc30f>.
- Xia, W., Rao, Q., Deng, X., Chen, J., Xie, P., 2020. Rainfall is a significant environmental factor of microplastic pollution in inland waters. *Sci. Total Environ.* 732, 139065.
- Xu, H., 2006. Modification of normalised difference water index (NDWI) to enhance open water features in remotely sensed imagery. *Int. J. Remote Sens.* 27, 3025–3033.
- Xu, Y., Yuan, Q., Zhao, C., Wang, L., Li, Y., Ma, X., Guo, J., Yang, H., 2021. Identification of nitrate sources in rivers in a complex catchment using a dual isotopic approach. *Water* 13, 1–19.